

Investigation of the Erosion phenomenon in
high current, high pressure gas discharges

J.E. Gruber R. Suess

IPP 4/72

December 1969

INSTITUT FÜR PLASMAPHYSIK
GARCHING BEI MÜNCHEN

INSTITUT FÜR PLASMAPHYSIK**GARCHING BEI MÜNCHEN**

December 1969

Investigation of the Erosion phenomenon in
high current, high pressure gas discharges

J.E. Gruber R. Suess

The erosion measured as the loss of electrode material was determined in different spark gaps with planparallel electrodes. In the range from 50 to 300 kA and a corresponding total current conduction 50 Coulomb per discharge, the erosion in a 1,5 mm gap was found to be nearly two orders of magnitude higher than in a 13 mm gap at atmospheric pressure. The close electrode spacing was found to be responsible for the increased erosion rather than the gas pressure. Erosion values for an oscillatory current are given for Aluminium, Brass, Stainless Steel, Molybdenum, Tungsten and Tungsten-Copper alloy.

IPP 4/72

December 1969

Die nachstehende Arbeit wurde im Rahmen des Vertrages zwischen dem Institut für Plasmaphysik GmbH und der Europäischen Atomgemeinschaft über die Zusammenarbeit auf dem Gebiete der Plasmaphysik durchgeführt.

Investigation of the Erosion
phenomenon in high current,
high pressure gas discharges

J.E. Gruber, R. Suess

December 1969

Abstract

The erosion measured as the loss of electrode material was determined in different spark gaps with planparallel electrodes. In the range from 50 to 300 kA and a corresponding total current conduction between 1 and 50 Coulomb per discharge, the erosion in a 1,5 mm gap was found to be nearly two orders of magnitude higher than in a 13 mm gap at atmospheric pressure. The close electrode spacing was found to be responsible for the increased erosion rather than the gas pressure. Erosion values for an oscillatory current are given for Aluminium, Brass, Stainless Steel, Molybdenum, Tungsten and Tungsten-Copper alloy.

The bank capacity could be varied from 7,2 to 36 μF , with a maximum charging voltage of 18 kV of each bank half, which resulted in a maximum driving voltage of somewhat

1. Introduction

The reliability and life of high current spark gaps depend mainly on the condition of the electrode surface and tracking of the insulator surfaces exposed to the spark plasma. The spark erosion causes successive destruction of the switch electrodes and eroded material is deposited at the neighbouring insulator surfaces.

Different physical mechanisms are responsible for the complex erosion process. The spark channel is highly confined to discrete spots at the electrode surface, and it causes there fast intense heating. In consequence melting and vapourization of electrode metal combined with explosive blowout of metal occur.

A theoretical calculation of the heating process and of the formation of vapour jets is only possible by application of a simplified model of the rather complex multistage process (Ref. 1, 2, 3, 4). Experimentally found erosion values at small currents agree better than those found at high pulse currents (Ref. 5, 6, 7, 8) and considerable differences between predicted and measured values were experienced.

The enhanced development of high current low inductance spark gaps for controlled thermonuclear research necessitated the investigation of the erosion in high pressure systems with closely spaced electrodes. Our main interest was to find the erosion rate in dependence of the conduction period, the current, the gas pressure and gap distance for a selection of technical interesting metals for application in high current

low inductance spark gaps. Besides the direct measurement of the eroded mass of electrode metal for a limited set of parameters of gap distance, gas pressure and conduction ratings, a series of photographic pictures of electrode surfaces exposed to high current discharges as well as the spark channel itself were taken to obtain further information for the basic understanding of the erosion process.

2. The Experimental Apparatus

The test electrodes were mounted in an open air spark gap I as shown in Fig. 1a for most of the 13 mm, 1 ata measurements. The spark gaps II and III as shown in Fig. 1b and 1c allowed operation at higher gas pressures up to 7 ata (1 ata refers to atmospheric pressure).

The test gap II was specially designed for operation in the capacitor bank EROS I, in which the spark gap had to withstand only pulse voltage. Up to five gaps could be operated at once in this arrangement. Due to the small spark gap volume of gap II enhanced contamination of the insulation and electrode surface was experienced at high Coulomb ratings. Also a burn-off and deposition of sputtered insulation particles at the electrode surface was observed. This caused a considerable spread in the measured erosion. Yet the use of the series arrangement with these gaps had the advantage that, by means of an overvoltage triggering, the gaps could be fired at different p.d - values, at constant gap voltage. Thus, it was possible to measure the influence of varying gas pressure on the erosion at a constant gap width and at constant Coulomb rating.

The circuit for the test battery EROS I is shown in Fig. 2. The bank capacity could be varied from 7,2 to 36 μ F, with a maximum charging voltage of 18 kV of each bank half, which resulted in a maximum driving voltage of somewhat

less than 36 kV after polarity conversion of one bank half. The polarity conversion was achieved by means of an additional conversion switch and an inductance as shown in the circuit diagram. A trigger pulse of 100 kV supplied to one of the intermediate gap electrodes allowed the ignition of the gaps below their DC breakdown voltage at different p.d values. A substantial number of testshots was carried out with the capacitorbank EROS II ($C = 15 \mu\text{F}$, $V_{\text{max}} = 40 \text{ kV}$) and to some smaller number in a 40 kV, high current bank, usually used for tests with ferrite decoupled spark gaps as reported elsewhere (made available by Mr.H.Wedler). The testgap III as shown in Fig. 1c, was used for most of the measurements at higher gas pressure. This gap had an extra large gas volume to avoid the previously mentioned difficulties of surface contamination by sputtered insulation particles. The current connections in the close gap neighbourhood were made symmetric with respect to the spark channel in order to minimize the arc blow out by magnetic field.

Considerable care had to be taken about the electrodes. These were manufactured from one piece in the case of Brass, Copper, Stainless Steel and Aluminium. With the other metals investigated: Tungsten, Molybdenum and Tungsten-Copper alloy, flat disks 8 mm thick, 30 mm Diameter, were soldered to a separate electrode holder, as can be seen from Fig. 1b. The accuracy in the measurement of the electrode weight was found to depend to a high degree on the cleanliness at the electrodes. In an initial test twenty carefully cleaned electrodes were weighted, stored away and weighted again the following day. The reproducibility in the weight using a precision balance with a maximum weighing capacity

of 1000 Grams and a resolution of 0,1 Milligram, was found to be several mg, in some cases even about 10 mg. In consequence all electrodes and the Stainless Steel jam-nuts were subjected to an electropolishing process to remove all sharp edges and spikes from the surface and thus reducing the amount of material wear during the gap mounting procedure. As a result the spread in the weight in consecutive measurements decreased to 1 - 2 mg. For evaluation of the effect of surface roughening in consecutive shots, the DC breakdownvoltage was recorded by a pen recorder which sensed the gap voltage via a high ohmic voltage divider. Observation of the spark channel growth was possible by use of a Beckman - Whitley Image converter camera with Polaroid Land back. With a shutter opening time of 10 Nanosec single photographs of the spark channel were taken. The electronic shutter was controlled by a Pulse Height Discriminator (developed by Mr.Hofmeister, electronic group) which gave the relation between the start of the current and the timepoint of shutter-opening. The Lens System Jena S, 180 mm, f 1:2,8 allowed a reproduction of the observed region in a magnified scale (2:1) on the photographic film.

3. Experimental Results and Comparison with published Data.

The great number of possible spark gap parameters made a preselection in the experimental parameters necessary in order to limit the experimental effort.

The goal of our work was:

- a) To find a comparison in the erosion for those metals appearing useful for application in high voltage high current spark gaps.

- b) To obtain data of the erosion in pressurized spark gaps and compare it with the erosion in atmospheric spark gap systems (some data for a limited number of metals has been published as discussed later).
- c) To contribute to the basic understanding of the very complex nature of the erosion process and to find a link between the material properties, the theoretical calculation and the observed erosion rate.

The following spark gap parameters were chosen:

The Spark Gap Geometry:

The planparallel gap with quasihomogenous field (for the 13 mm gap) and nearly homogenous field (for the 1,5 mm gap) offered the advantage of a small change in gap distance even during longer test runs. The change in gap breakdown voltage therefore could be contributed mainly to a change in surface condition by erosion.

The Gap Distance and Gas Pressure:

Two values representative for a spark gap with a DC breakdown voltage between 30 and 40 kV were chosen as follows:

For the atmospheric gap 13 mm and 1 ata (1 ata = 760 mm Hg)

For the pressurized gap 1,5mm and 6,5 ata.

No correction was made either for the barometric day by day variation or for the pressure lowering of the geological altitude of the location of the experiment. The influence

of these items have to our opinion only a second order influence (as will be seen later). For all pressure tests either synthetic bottled air (80% N₂ and 20% O₂) or dried and filtered pressurized air from the inhouse supply was used, the dewpoint of the later being below -50°C.

The Current-Waveshape and Pulselength:

A considerable number of experiments in CTR research utilize a sinusoidal waveshape. Therefore and also as a matter of convenience all tests were carried out with a damped sinusoidal current having a decay time constant $T = 2 L/R$ usually ranging between 50 and 200/usec.

The measured values of erosion have been plotted in dependance of the transported charge $Q = \int idt$ which allows comparison with published data in atmospheric gaps (Ref. 7, 8, 9). In Fig. 3 and 4 the eroded volume (derived from the measured loss in weight) has been plotted for all metals investigated for Q varying from 2 to 50 Coulomb per discharge.

Each point represents the arithmetic mean loss of both spark gap electrodes. With the oscillatory current no polarity effect could be found as expected.

Especially for Copper and Brass a discontinuity in the erosion curve was found. In the 13 mm gap Copper competes successfully with the high melting point metals Tungsten and Tungsten copper alloy. At about 5 Coulomb the erosion increases rapidly to settle further near values of Steel and Brass. It should be noted, that the slope of the curves besides this "change-over region" seems to be constant. Curves with a similar slope

proportional to the $\int i dt$ if the energy in the arc channel is made responsible for the heating. A different approach is the assumption that the ohmic loss in the metal itself provides the energy for the heating. The energy deposited

were obtained in the pressurized 1,5 mm gap (Fig.4) though the erosion there is considerably increased at the same current ratings.

Surprising is the behavior of Brass at low Coulomb values and it is there a successful competitor even for Tungsten. Remarkable poor is the behavior of steel. Brass also showed from 15 Cb upwards an increased erosion as we found for Copper in the atmospheric gap. It is obvious that only a changeover in the physical process can be made responsible for this and one could anticipate a similar behavior also for other metals possibly in a different range of test parameters as chosen here. Previously also Belkin (Ref.7) found a marked discontinuity in his curves for Copper at atmospheric pressure.

Most approaches so far for a theoretical erosion determination allow only for a heating process with consequent melting and evaporation (Ref. 6, 7), though a few explain the erosion as an explosion type process (Ref.2, 4). Taking into account the values of all the molten material, a too high erosion is derived at least at low current ratings. In reality only a part of the molten material will evaporate and be lost. If the heating process (i.e. the currentflow) lasts long enough, molten material also may be lost by a simple dripping off process. In the case of a high current density, prevailing in high current spark discharges, the extreme fast heating of a spot like zone leads to the generation of a high pressure metal gas vapour (up to 10^3 ata acc. Ref.9) with explosion type jets erupting from the electrode surface. In addition liquid metal also may be blown out by the expansion of the heated gas

neighbouring the electrode surface. Thus we found in the pressurized spark gap an erosion rate which is in some cases up to two orders of magnitude greater than in the 13 mm atmospheric gap. In Fig. 5 the measured erosion for Copper is compared with values obtained by Belkin (Ref. 7) and the theoretical values for the molten amount. Belkins model of surface heating assumes that the energy deposited in the spark channel i.e. $E = \int u_{arc} \cdot i dt$ is only responsible for the heating of the material. Thus the molten material becomes proportional to $\int i dt$, if the arc drop voltage is assumed to stay constant.

Further it was of interest to find out which role the gas pressure itself plays, i.e. whether a discharge channel in a higher gas pressure leads to increased erosion. With the earlier described capacitorbank EROS I it was possible to initiate a spark channel at constant gap distance but with varying gas pressure. This measurement is presented in Fig. 6. Though there is an increase in erosion for Copper by a factor of two, the other metals stayed with unchanged erosion over the whole pressure range. In comparison with the previous results in which Copper had an increased erosion by a factor of 8,3 in the small 1,5 mm gap (6,5 ata) with respect to the 13 mm gap (1 ata), it can be concluded, that the gas pressure has only little effect on the erosion rate. As the transient pressure in a gas discharge may reach values as high as 10^3 ata, it is obvious that the increase in surrounding gas pressure from 1 to 6,5 ata can have no marked effect. A further testserie was made to establish the erosionrate either in favour of the amount $\int i dt$ or $\int i^2 dt$.

As pointed out previously the molten amount of metal is proportional to the $\int i dt$ if the energy in the arc channel is made responsible for the heating. A different approach is the assumption that the ohmic loss in the metal itself provides the energy for the heating. The energy deposited

in this case equals $\int \rho i^2 dt$ (ρ is the specific resistance of the metal) and consequently a relation $M = k \cdot \int i^2 dt$ can be derived.

The experimental verification of one of the two dependences turned out to be rather difficult. The pulse generator has to deliver a constant charge flow $Q = \int i dt$ for a current varying in some suitable range i.e. in our case between 10 and 200 kA. The best approach would be a pulse forming network (LC network) delivering a square wave current with variation both of peak current and pulse length. We tried to obtain a solution by using the available capacitor bank in which different current levels were obtained by altering the capacitance and the inductance (load coil). In order to obtain a constant $\int i dt$ the resistance had also to be adjusted. In Fig. 7 the erosion rate has been plotted as obtained this way for Brass and Tungsten Copper for varying currents from 40 to 180 kA. The result does not prove that the erosion is independent of the current value, or that a dependence exists for $\int i dt$ alone. Rather it seems that there is a weak dependence on the current as well. This has to be expected as the energy released from the arc channel is much higher than the ohmic loss amount in the metal.

This means that plotting the erosion in dependence of $\int i dt$ as carried out by most workers in this field characterises closest the phenomenon.

A dominant role plays the surface condition for a multishot spark gap application. In Fig. 8 and 9 typical destructions are shown as obtained in the 1,5 mm gap at 6,5 ata for

either 100 shots with 4,4 Coulomb (60 kA) resp. 1 shot at 46 Coulomb (170 kA). Deep melting zones can be seen for Copper and Brass, but also for Tungsten. A similar rough surface structure was observed for Stainless Steel and in an excessive way for Aluminium. Though there was considerable melting found with Brass, only spurious signs for a blowout were found on the surrounding walls. It should be noted that this metal gains finally a smooth overall surface. This suggests that Brass erodes mainly by vaporization from spots which are distributed over a greater surface area. Copper which has a quite low erosion at low Coulomb values (in the 13 mm gap) suffers from blowout of liquid droplets. A considerable amount of splashed Copper was found at the neighbouring insulation parts. Similar is the surface structure if Tungsten and Tungsten-Copper are compared with each other. The presence of a low melting point metal (e.g. Zinc in Brass and Copper in Tungsten Copper) favours an early boiloff-process and therefore the generation of a more distributed area of arc spots is enabled. This seems to be the main reason for the lower erosion rate observed for the alloys in some cases.

Interesting is the different amount of surface melting in the wider gap (13 mm) with respect to the shorter (1,5 mm) gap, as shown for Brass in Fig. 10.

During the use of a spark gap the surface condition is continuously varying as spikes and crater edges are generated in one shot and possibly are then removed by erosion in the following shot. The suitability of a certain metal for use in a pressurized system with small gap distance

will depend largely on the surface variation in continuous shots. A measurement of the DC breakdown voltage will reflect the surface condition. In Fig. 11 the DC breakdown voltage of Brass, and the Tungsten alloys Tuconit and Heavy metal are compared. A pen recorder in conjunction with a high ohmic voltage divider continuously recorded the breakdown voltage. The Data presented give the relative change in the mean breakdown voltage in twenty consecutive shots after a suitable number of preconditioning shots. It should be noted that the absolute value of the breakdown voltage for the different metals is not the same. Usually the "smoother" metals Tuconit and heavy metal can have a mean breakdown voltage which is a few percent higher than that of Brass after the preconditioning process. Finally we carried out an optical observation of the spark channel by means of an Image Converter Camera.

The object of this test was to find more information about the early time history of the erosion process. The electronic shutter of the image converter camera allowed to take short time (10 nsec) exposures of the spark channel. The time relation between the start of the current and the time point of shutter opening could be varied by means of a pulse height discriminator and a time delay unit. The pulse height discriminator has been controlled by the pulse of a pick - up coil near the spark channel. The discriminator gave a well - defined short risetime pulse to start the delay unit. The electronic shutter was triggered by the delayed pulse from the delay unit.

A 180 mm lens focussed the spark gap image into the Image Converter screen in a 2 : 1 enlarged scale. The tube picture then was photographed by a standard camera with Polaroid back. The pictures obtained by this method allowed the

observation of the spark channel at different time points. The resolution was sufficient to distinct metal vapour break-out.

In Fig. 12 the pictures of the discharge in a gap with either Brass, Copper or Tungsten-Copper electrodes are shown. As the Image Converter Camera allowed only one exposure per discharge, the series shown are those from consecutive shots. No measurable variation of the spark channel radius could be found in pictures from different shots having the same timedelay of shutter opening. The pictures show two timeregions for all three electrode materials. The early phase shows the existence of a uniform hot channel which is formed from hot gas plasma. The term uniform refers to the luminosity of the channel only, i.e. the existence of a high pressure shockwave at the channel outside and the low pressure region in the channel center, as is widely accepted, could not be found with the photographic technique applied in this experiment. In this phase the discharge channel is confined to a small area of some mm^2 and the damage to the electrode surface results as a bombardment by charged particles rather than by a thermodynamic process. With the current involved in our tests region is typical a short (sub- μsec) time region.

In phase II surface melting and explosion type ejection of metal vapour but also liquid portions do occur. In the pictures this is seen as a brighter region starting at the electrode surface and growing like a pyramide from both electrodes, the cathode and the anode. The pictures show the onset of a metal vapour cloud about 3,5 μsec after

current initiation. The metal vapour breakout interrupts locally generated electron emission from hot spots and new spots will be generated at the channel circumference. A multiplicity of hot spots with concentration towards an annular zone has been reported by Sommerville (Lit. 10) even for much smaller currents (36 A) and the time to obtain distributed melting was also several μ sec. In this second phase a severe electrode damage occurs as a combination of melting, vapourization and explosion type blow-out of metal vapour and also liquid material. The erosion resistance of a certain metal or alloy therefore is closely linked to the ability to generate a sufficient metal vapour cloud which in consequence leads to a shifting of the hot emission centres and thus avoiding a deep burn-in at a concentrated area. A similar effect is thus obtained as is utilized in power arc switches where the arc root is continuously shifted by magnetic or gasdynamic action to prevent local electrode burn.

The spark channel photographs for Brass, Copper and Tungsten-Copper show, that (in the time regime investigated) the spark channel region is about the same for all three metals. The different areas of surface melting derived from the surface photographs, as shown earlier, indicate, that a major part of erosion takes place at later times, even after the heating current pulse has passed, as the action of the present hot gas expansion. Fig. 13 shows the spark channel growth versus time. The surface roughness depends on the depth of melting, which in consequence is crosslinked to the hotspot concentration. The different behavior of pure metals and alloys can be explained : The presence of a metal with low melting point and extensive vapour generation (e.g. Zinc in Brass, and Copper in Tungsten-Copper) leads to a

back. The pictures obtained by this method allowed the

continuous hot spot transfer and a local deep melting is avoided.

The ideal material combination therefore is a high melting point metal matrix with good mechanical crosslinking and a filler metal with low melting and vapourization point. A further point of importance seems to be the electrical conductivity. The metals Molybdenum and Stainless Steel though having higher melting and boiling point than Copper showed poor erosion resistance as can be seen from Fig. 3. Aluminium is an exception, the extrem low melting point (657°C) and its poor oxidation resistance must be made responsible for the increased erosion.

4. Conclusions

The experimental measurement of the eroded volume from the electrode surface of different metals revealed some inconsistencies with theories published in the past. A deviation of the experimental results from the theoretical predicted values was found to be in some cases about two orders of magnitude. The closest agreement could be established with the calculated volume of totally molten material, which gives the upper limit of observed erosion (Theory by Belkin, Lit 7). The erosion phenomenon was investigated only with respect to a change in surface condition of the electrodes in open and pressurised spark gaps. At high coulomb ratings and for the severe duty in a closely spaced electrode system, Tungsten-Copper showed superior behavior both from the aspect of eroded volume and change in surface condition. The probes from three different manufacturers gave similar results, though Heavy

metal is inferior to Elmet-Rotung p (80% Tungsten, 20% Copper). It might be anticipated that excellent erosion resistance can be expected from similar compound metals e.g. Tungsten-Silver, Tungsten-Thorium etc. At lower Coulomb ratings and in open air spark gaps Copper and Brass may give sufficient erosion resistance. In sealed-off systems with closely spaced insulation surfaces other factors then investigated here may govern the suitability of a certain metal. It has been found e.g. for Copper, that the layer deposited at the insulation surface has a shiny reddish appearance, obvious consisting of Copper particles. In time this may lead to a conducting layer. With Brass this layer, due to the presence of Zinc oxide, is possibly less harmful. Further investigation of this deposition problem, which is also part of the erosion phenomenon is necessary. Also still open is the polarity effect at high coulomb ratings and the influence of different gases.

5. References:

- 1) Llewellyn-Jones F., Brit.Journ. of Appl. Physics
Vol.1, No.3, March 1950, pp.60-65
- 2) Finkelburg W., Physical Review, Vol.74, No.10
1948, pg. 1475
- 3) Cundall C.M., Craggs I.D., Spectrochimica Acta, 1955,
Vol. 7, pp. 149-164
- 4) Mandelstam S., Spectrochimica Acta, 1959,
pp. 255-271
- 5) Wilson W.R., Proc. AIEE, Aug.1955, pp.657-664
- 6) Il'in V.E., Lebedev S.V. Sov. Phys., Techn. Physics,
Vol.7, No.8, Febr.1963, pp.717-721

- 7) Belkin G.S., Kiselev V.Y., Sov.Phys.Techn.Physics,
Vol.11, No.2 Aug.1966
pp.280-283
- 8) Menke H., Schroeder K.H. Elektrotechn. Zeitschrift A.,
Bd.87, 1966, Heft 10, pp.323-328
- 9) Rakhovskii V.I. Sov.Phys.Techn.Physics, Vol.10,
No.12, June 1966, pp.1707-1709
- 10) Sommerville J.M., Grainger C.T., British Journ. Appl.Phys.
Vol.7, March 1956, pp.109-111

6. Acknowledgements:

The work was performed in the Institut für Plasmaphysik GmbH.,
Abteilung Technik. The authors wish to express their thanks
to the Wissenschaftliche Leitung for the permission to carry
out the experiments and Mr. K.H. Schmitter for the conti-
nuous assistance and helpful discussions. Our thanks go to
Dr. Weichselgartner and Mr. Spitzer (electropolishing of
electrodes), Mr. Häglsperger and Mr. Dietz (Vacuum soldering
of electrodes) and Mr. Hauck for the preparation of the ex-
periment.



c) Pressure-tank Gap III

IPP

Abt.

Technik

Fig. 1 Geometry of Testgaps

I, II and III

G 001

7. List of Figures

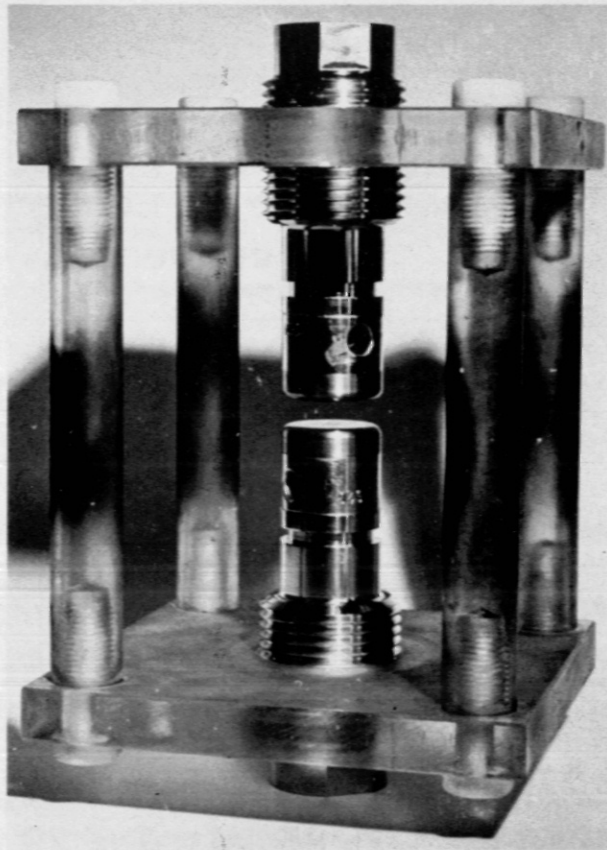
- Fig. 1 Geometry of testgaps I, II and III
- Fig. 2 Testbattery EROS I
- Fig. 3 Erosionrate for different electrodemetals
(13 mm gap, 1 ata gas pressure)
- Fig. 4 Erosionrate for different electrodemetals
(1,5 mm gap, 6,5 ata gas pressure)
- Fig. 5 The erosion of Copper
- Fig. 6 The effect of gaspressure on the erosionrate
in a 2 mm gap ($Q = 7$ Cb const.)
- Fig. 7 The erosionrate at a constant Coulomb rating
but varying current
- Fig. 8 Surface destruction after 100 discharges at
4,4 Cb, 60 kA
- Fig. 9 Surface destruction after 1 discharge at 46 Cb,
170 kA
- Fig.10 Surface melting in a 1,5 mm and in a 13 mm gap
- Fig.11 Change of DC breakdown voltage in consecutive
discharges
- Fig.12 Spark channel growth photographed with an Image
Converter Camera in a 10 mm gap
- Fig.13 Increase of spark channel radius during one
discharge

3) Cundall C.M., Craggs I.D., Spectrochimica Acta, 1955,
Vol. 7, pp. 145-164

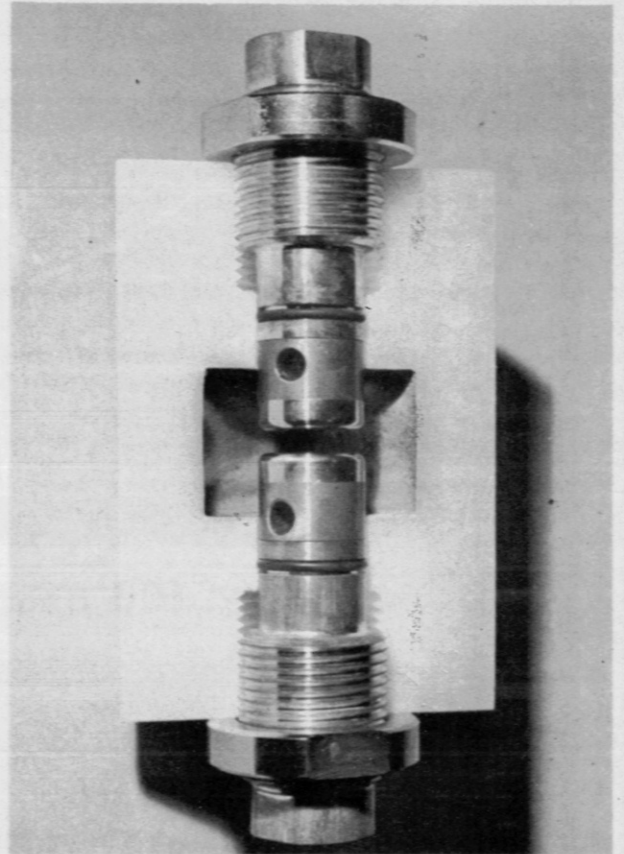
4) Mandelstam A., Spectrochimica Acta, 1959,
pp. 255-271

5) Wilson W.R., Proc. AIEE, Aug. 1958, pp.657-664

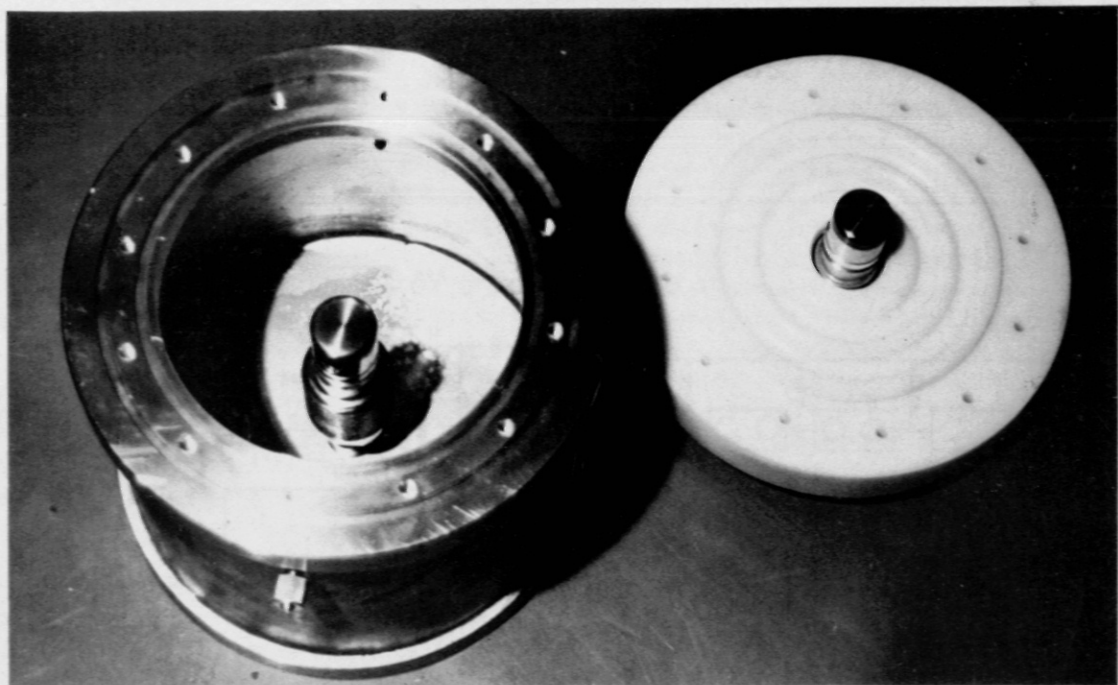
6) Il'in V.E., Ledevy S.V. Sov. Phys., Techn. Physics,
Vol.7, No. 8, Feb. 1963, pp.717-721



a) Open air Testgap I

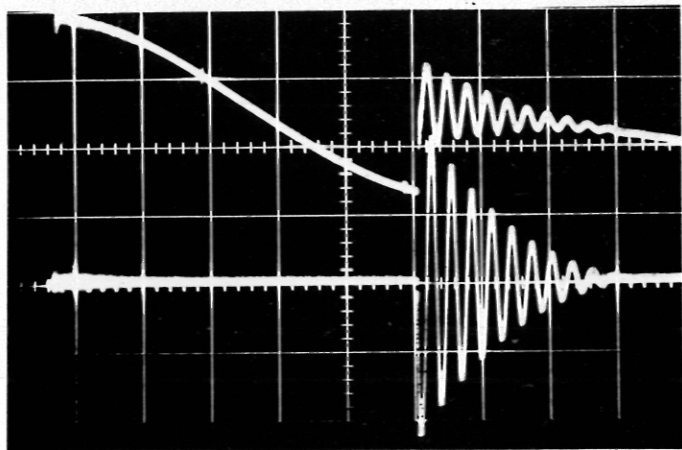


b) Pressurized Testgap II



c) Pressure-tank Gap III

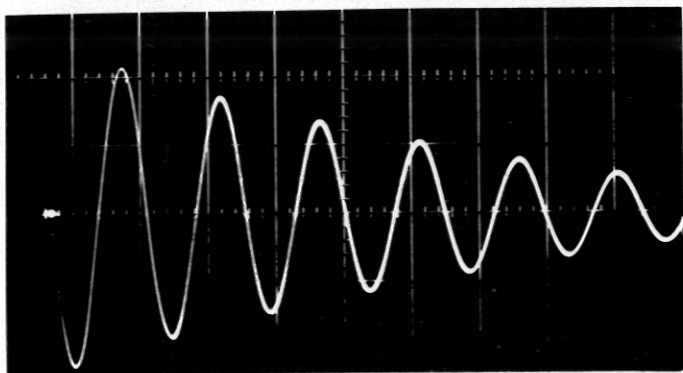
↓ 100 kV Triggerpulse



— Voltage at Converter - condenser

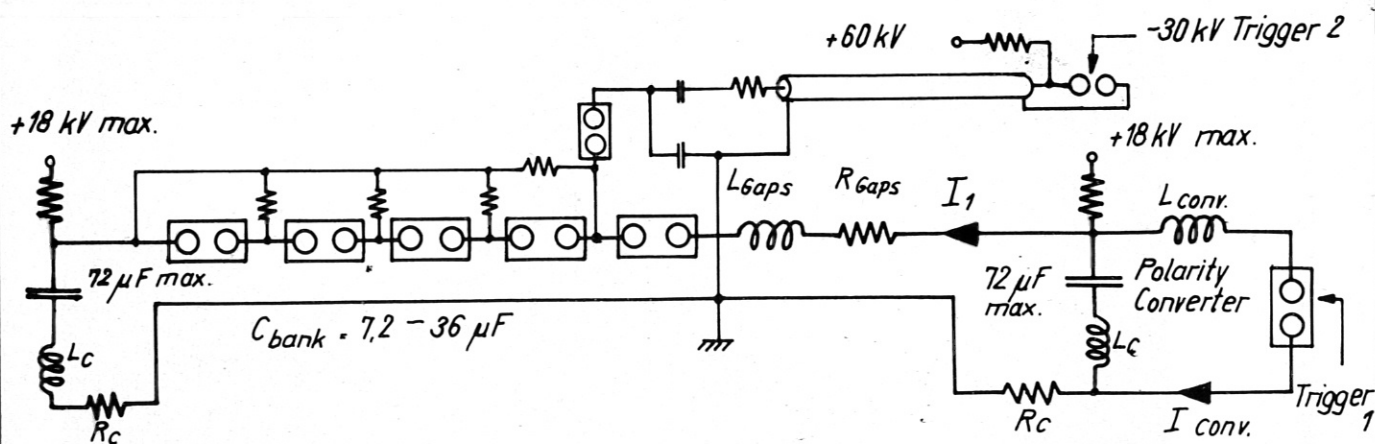
— Current I_1 in Testgaps

100 $\mu\text{sec/div}$ →



Current I_1 in Testgaps
 $\hat{I}_1 = 85 \text{ kA}$, $\tau = 29 \mu\text{sec}$
 $Q = 7,9 \text{ Cb}$, $U_{\text{bank}} = 28 \text{ kV}$

20 $\mu\text{sec/div}$ →



Circuit diagram

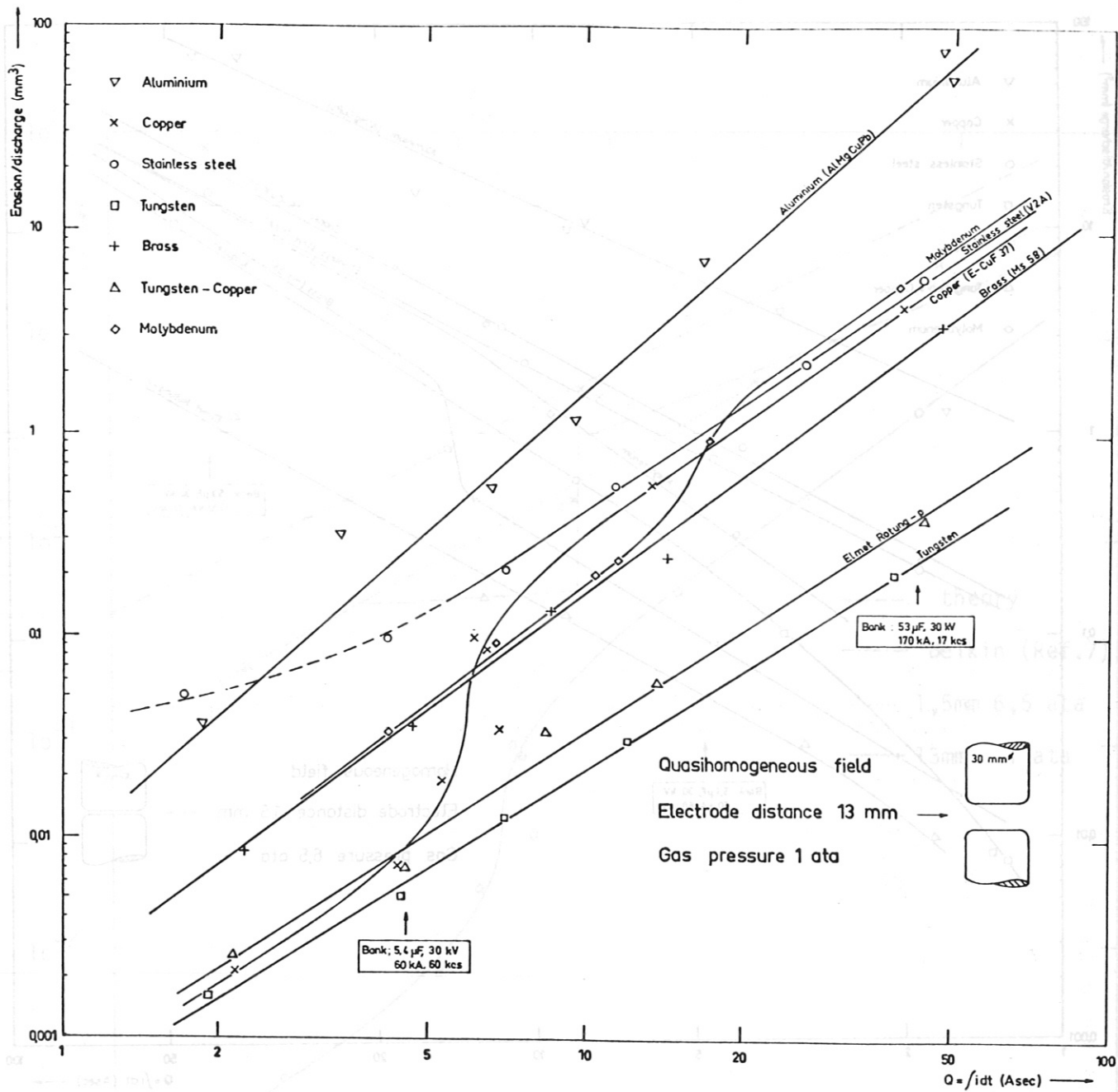


Fig. 5 The erosion of Copper.

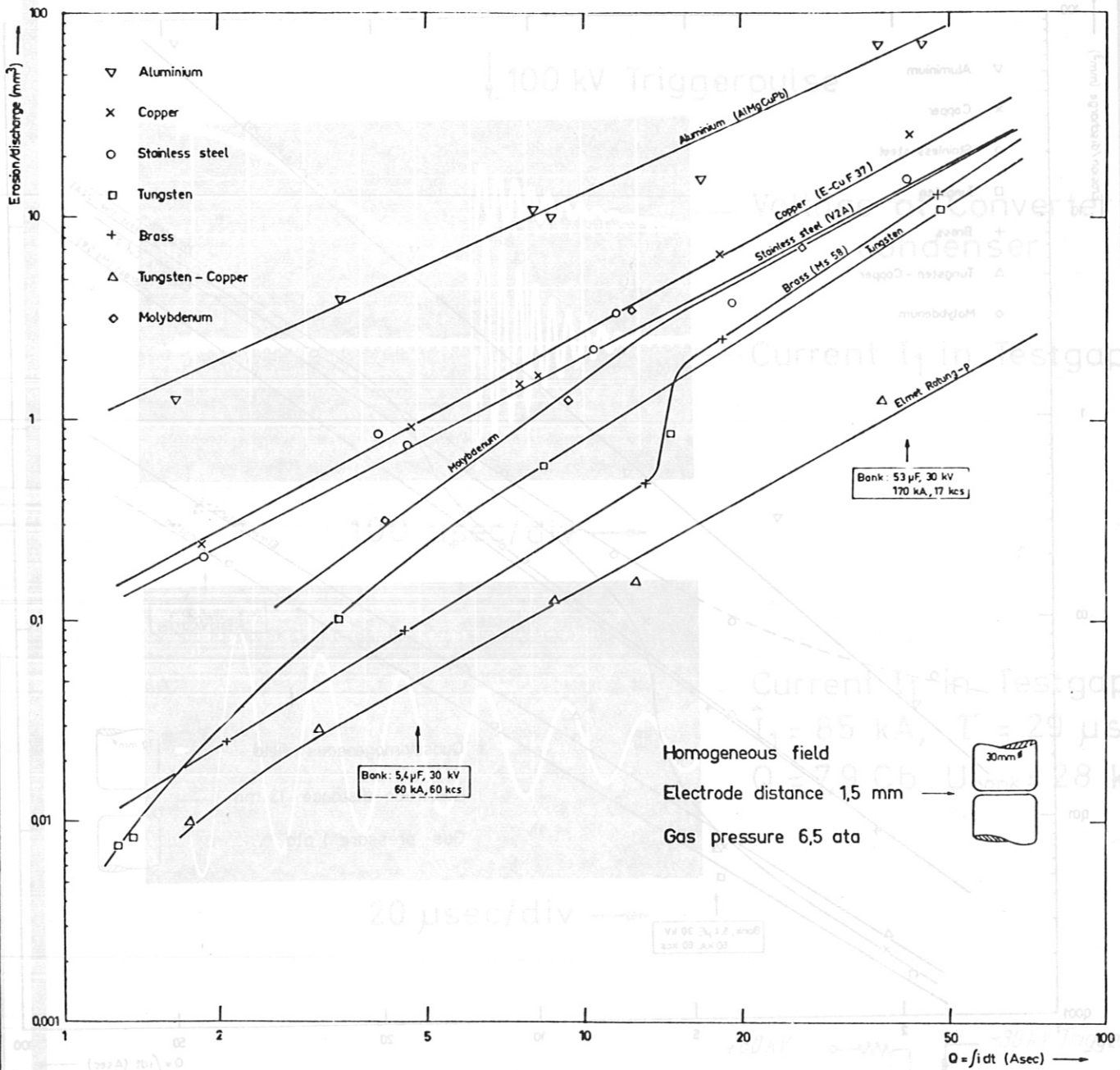


Fig.4 Erosion rate for different electrode metals (1,5mm, 6,5 ata)

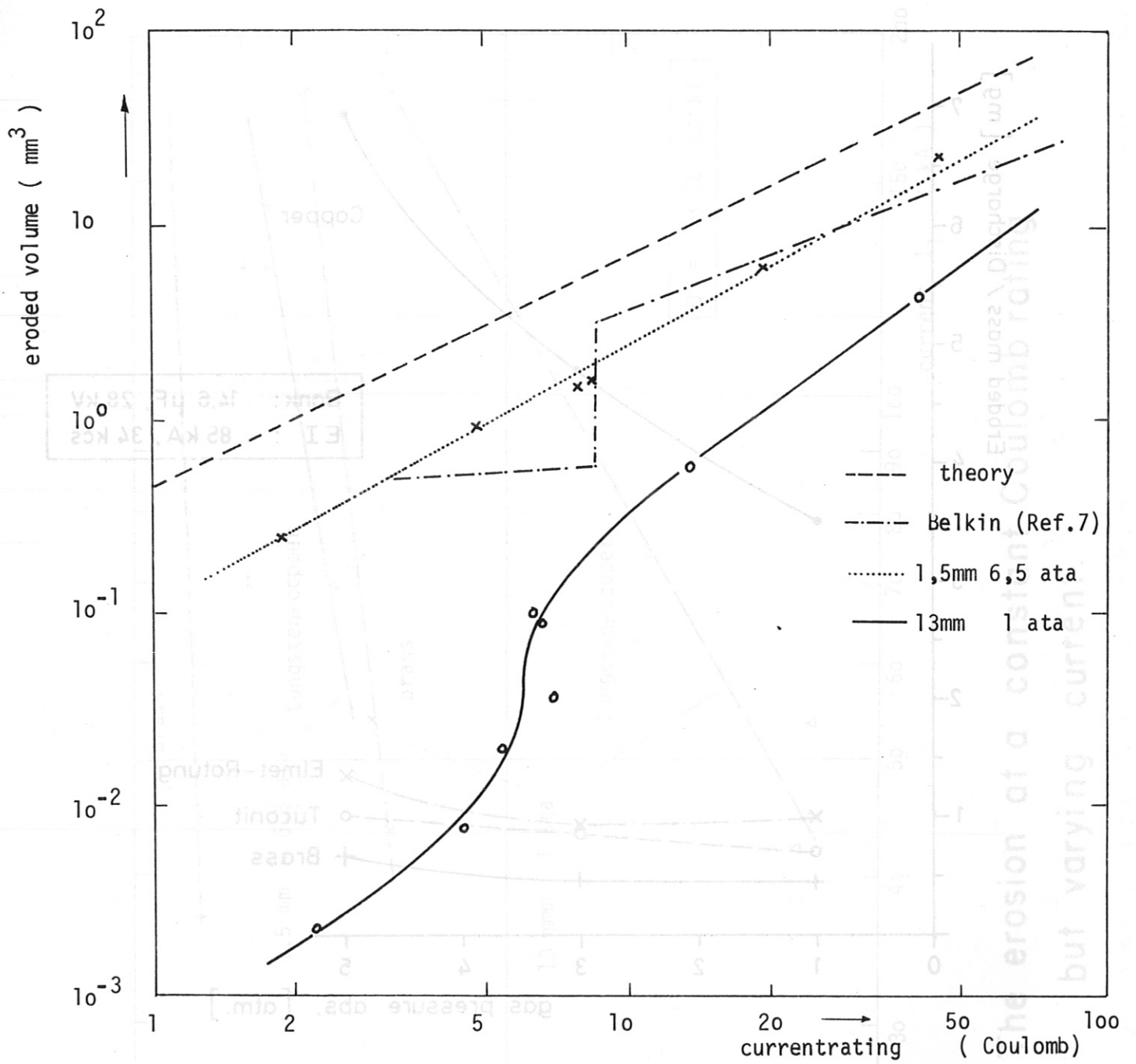


Fig. 5 The erosion of Copper.

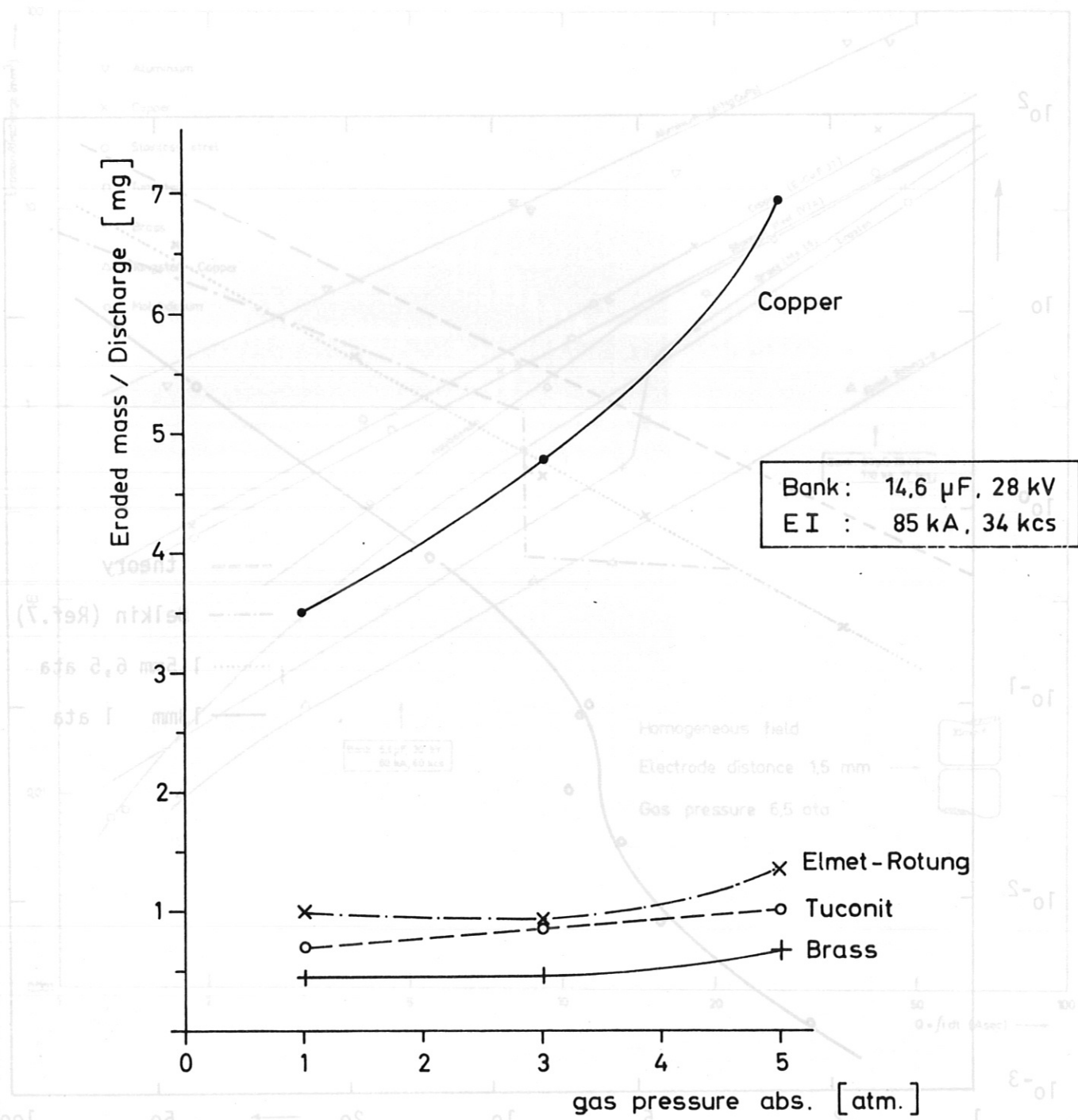


Fig. 6 Effect of gas pressure on erosion rate in a 2 mm gap electrodes 30mm diam., $Q=7Cb$ const.

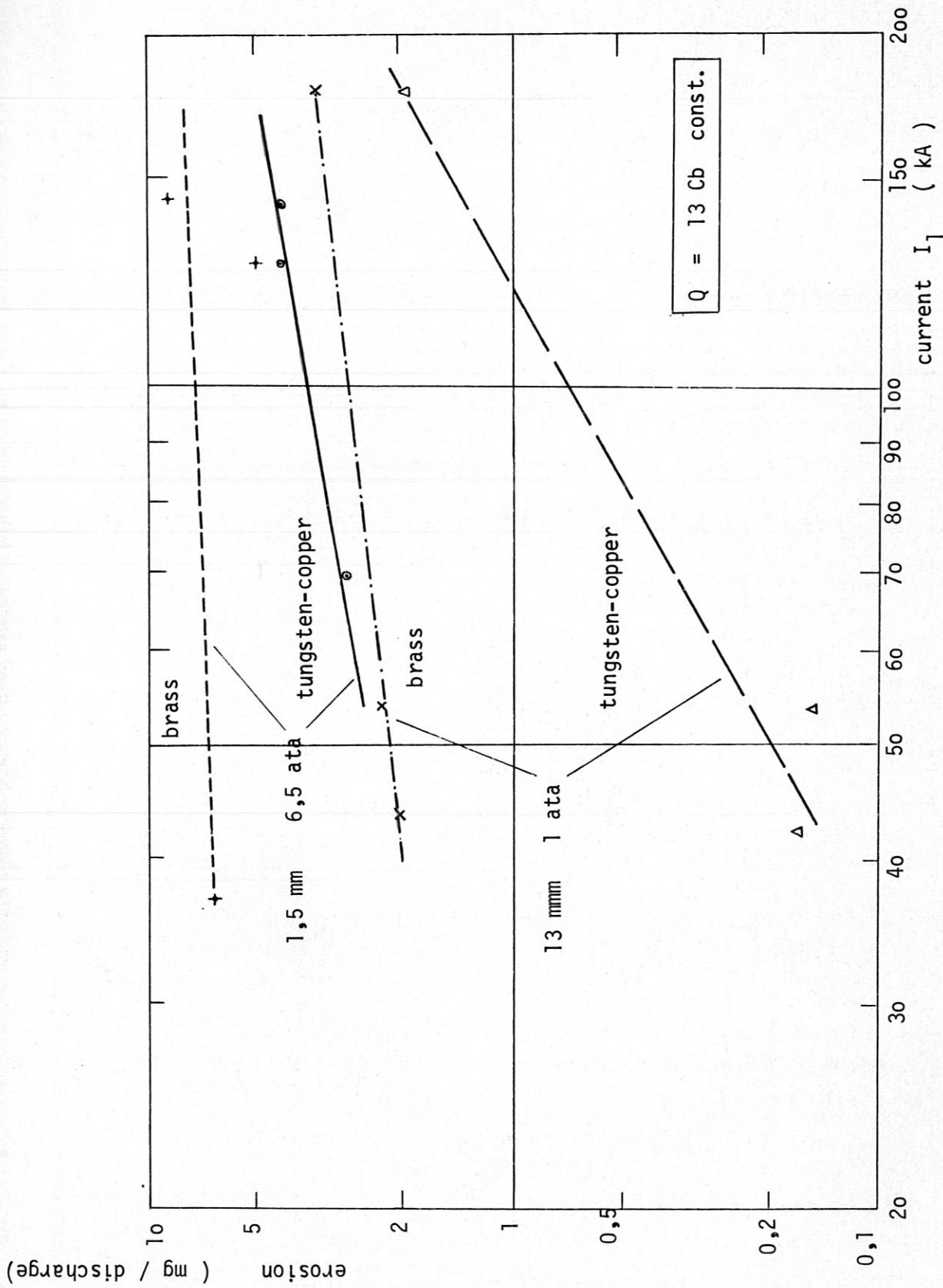
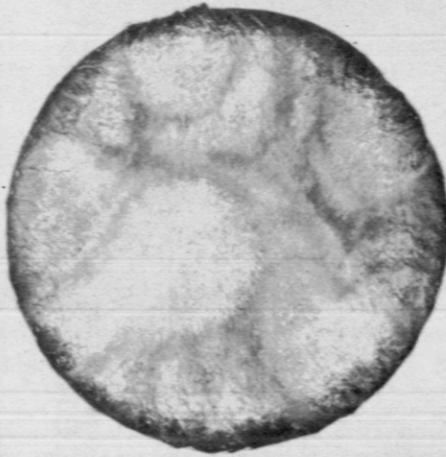
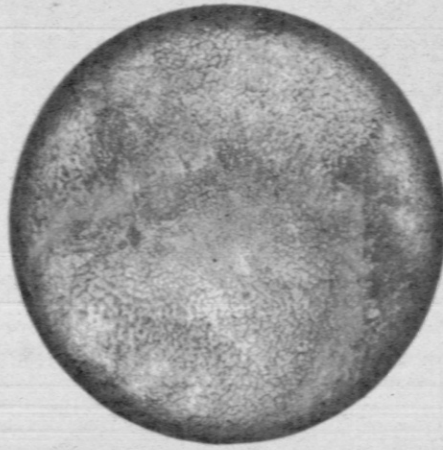


Fig. 7 The erosion at a constant Coulomb rating but varying current.



Copper



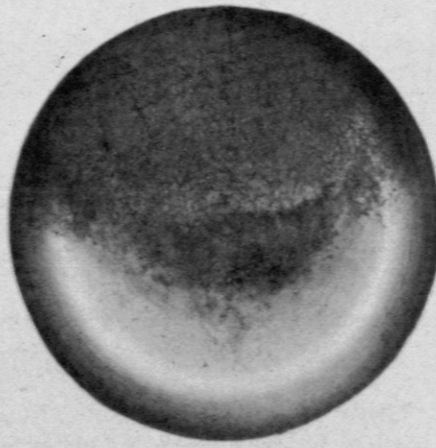
Brass
(Ms 58)



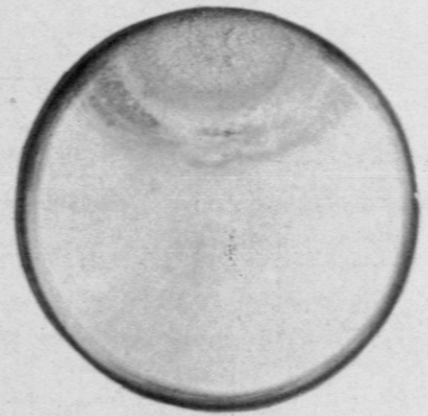
Tungsten



Heavy Metal



Tuconit



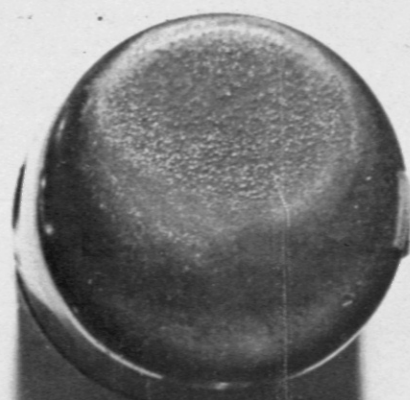
Elmet-Rotung

(Tungsten - Alloys)

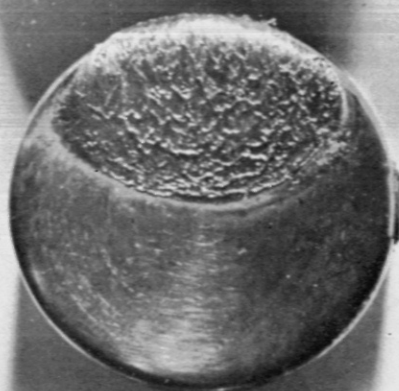
Testgap III , 1,5 mm Gap , 6,5 ata .



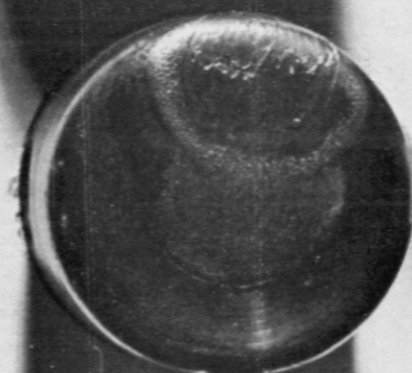
F79



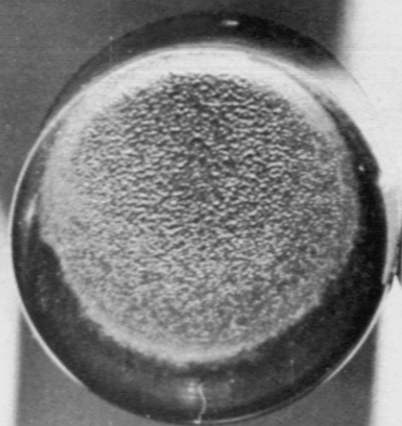
F83



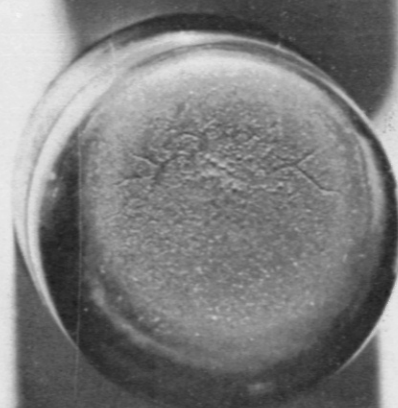
F80



F85



F81



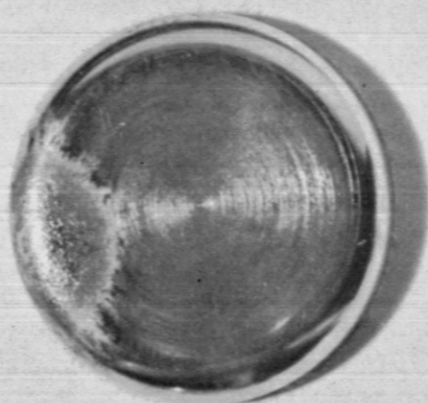
F84

Brass
Copper
Heavy Metal

Elmet - Rotung - P
Tungsten
Tuconit

Testgap III, 1,5mm Gap, 6,5 ata .

4,4Cb
60kA



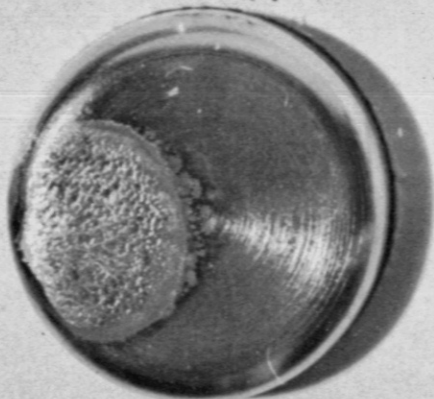
13mm
1ata

46Cb
170kA



13mm
1ata

4,4Cb
60kA



1,5mm
6,5ata

46Cb
170kA



1,5mm
6,5ata

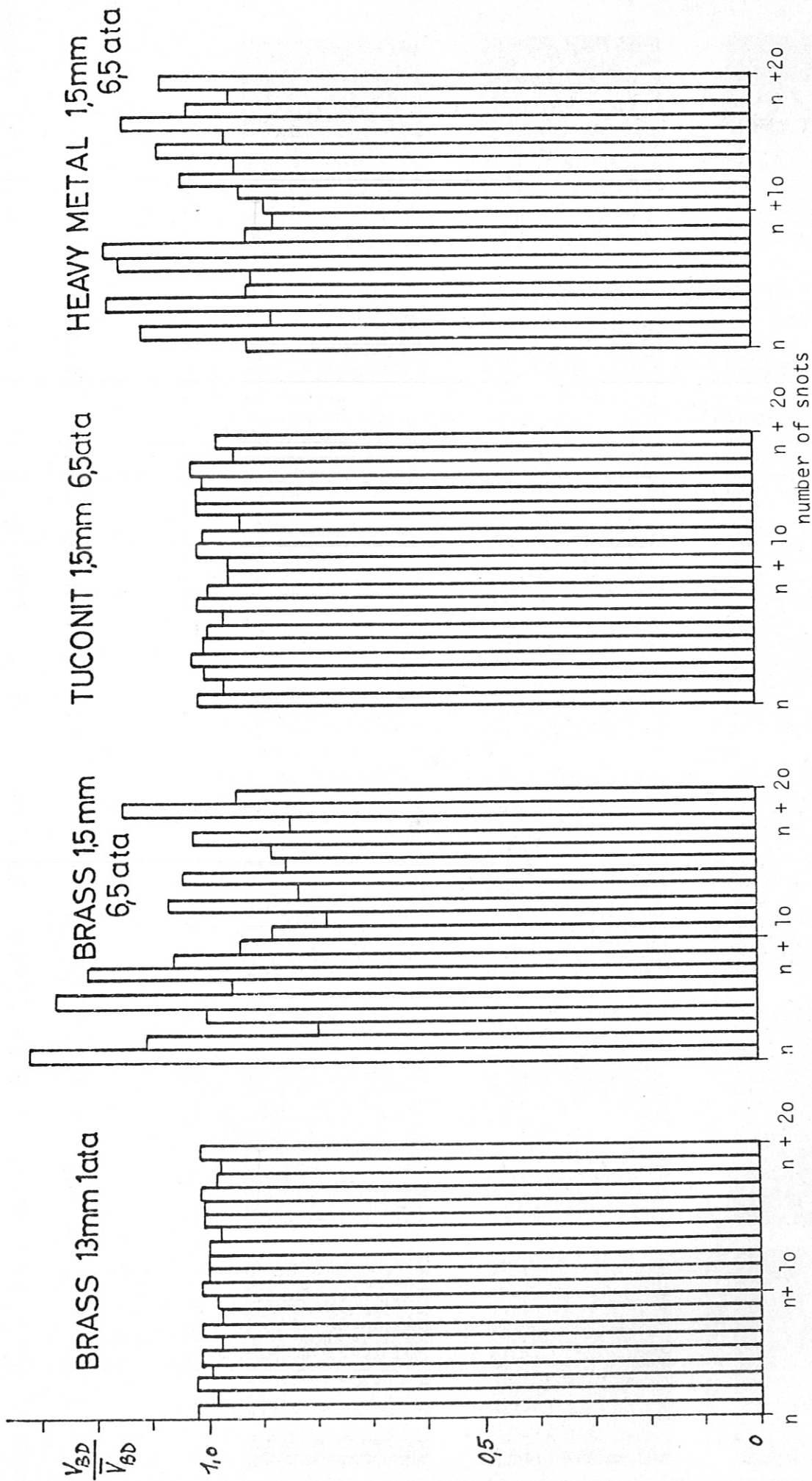


Fig.11 Change of statical breakdown voltage in consecutive discharges

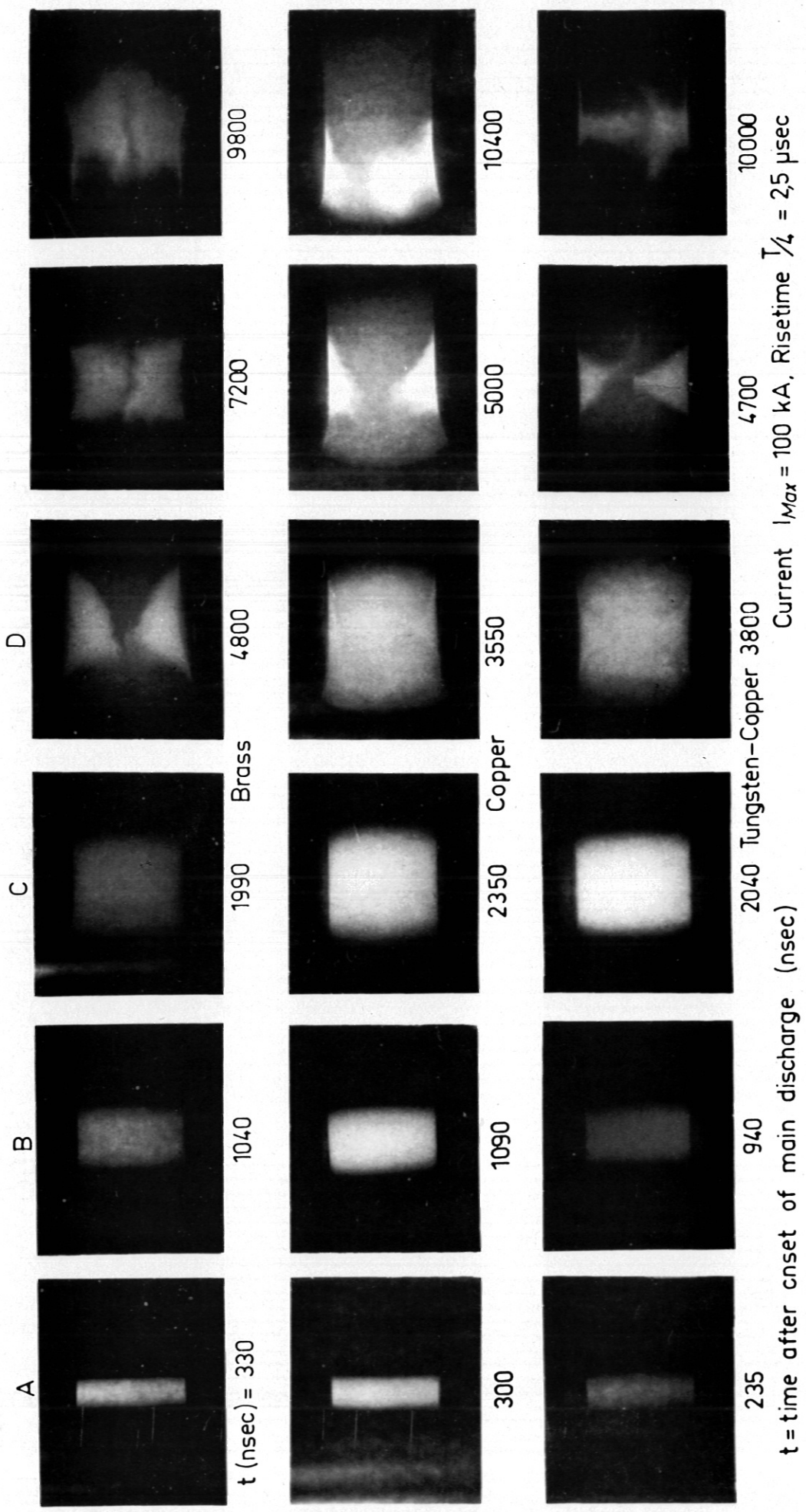
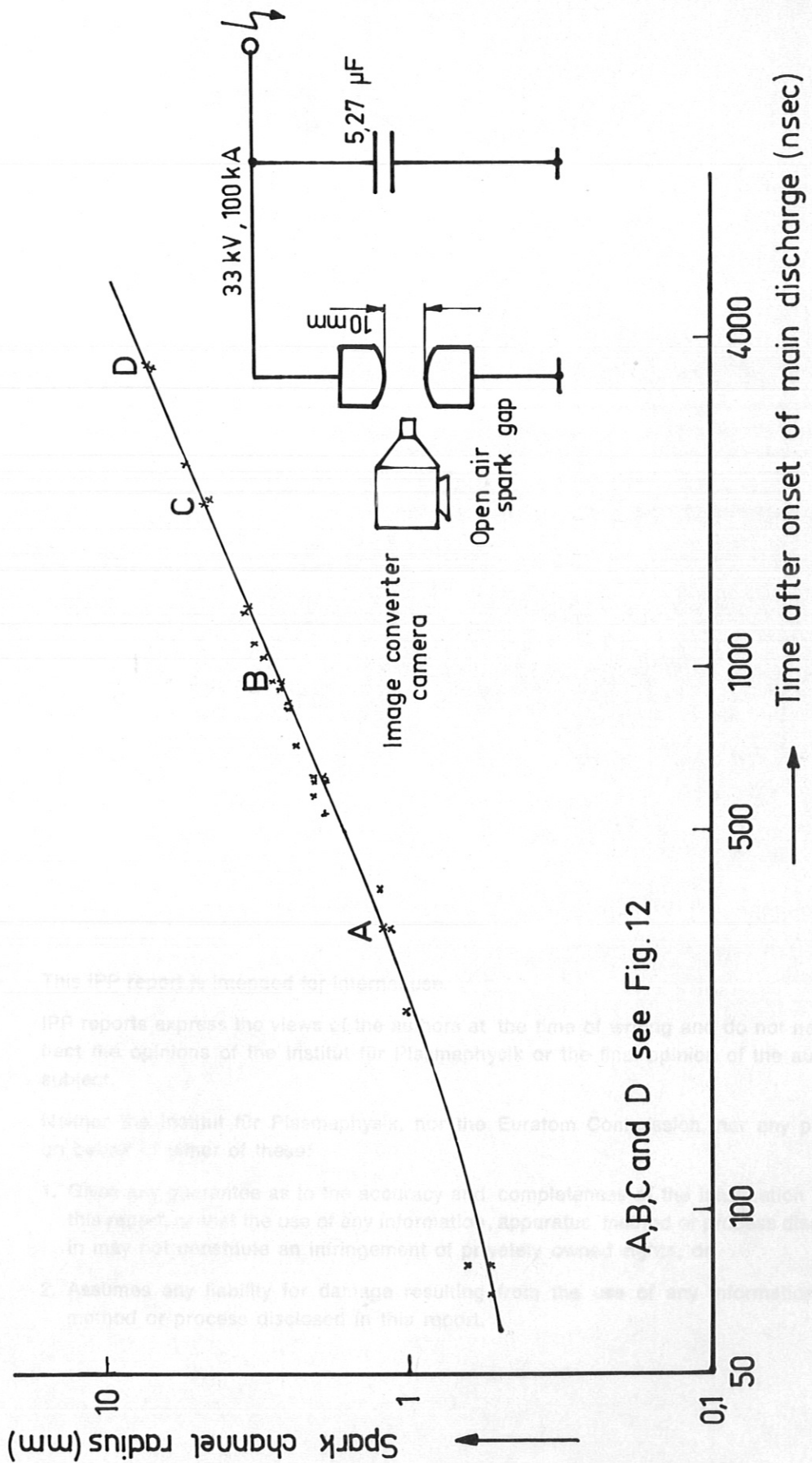


Fig.12 Spark channel growth photographed with an Image converter camera in a 10 mm gap



A, B, C and D see Fig. 12

Fig. 13 Increase of spark channel radius during one discharge